VOLUME 71, NUMBER 13 JOC Perspective JUNE 23, 2006

Investigations of Pd-Catalyzed ArX Coupling Reactions Informed by Reaction Progress Kinetic Analysis

Jinu S. Mathew,[†] Martin Klussmann,[†] Hiroshi Iwamura,[†,‡] Fernando Valera,[§] Alan Futran,[§] Emma A. C. Emanuelsson,[†] and Donna G. Blackmond*[,†,§]

Department of Chemistry and Department of Chemical Engineering and Chemical Technology, Imperial College, London SW7 2AZ, United Kingdom

d.blackmond@imperial.ac.uk

Received November 21, 2005

This Perspective highlights how the methodology of reaction progress kinetic analysis can provide a rapid and comprehensive kinetic profile of complex catalytic reaction networks under synthetically relevant conditions in a fraction of the number of experiments required by classical kinetic analysis. This approach relies on graphical manipulation of the extensive data sets available from accurate in situ monitoring of reaction progress under conditions where two concentration variables are changing simultaneously. A series of examples from Pd-catalyzed coupling reactions of aryl halides demonstrates how a wealth of kinetic information may be extracted from just three experiments in each case. Even before proposing a reaction mechanism, we can determine reaction orders in substrates, propose a resting state for the catalyst, and probe catalyst stability. Carrying out this kinetic analysis at the outset of a mechanistic investigation provides a framework for further work aimed at seeking a molecular-level understanding of the nature of the species within the catalytic cycle. To be considered plausible, any independent mechanistic proposal must be shown to be consistent with this global kinetic analysis.

Introduction

Twenty-five years ago, Halpern reviewed the role of transition-metal complexes in catalysis, an area of research that at the time was itself only about 25 years old.[1] That review highlighted the mechanistic elucidation of the homogeneous hydrogenation of olefins using Wilkinson's catalyst and using cationic Rh complexes with chelating chiral phosphine ligands. It is remarkable that today these two examples remain among the most comprehensive kinetic and mechanistic analyses ever accomplished on catalytic reaction networks. In addition to their fundamental scientific significance, these examples have provided us with a valuable pedagogical approach to such investigations. Two "take-home lessons"[2] from this work still stand us in good stead and are worth repeating: (a) what you see may not be what you get within a catalytic cycle; that is, observable or isolable species can be confirmed as true catalytic intermediates *only* via kinetic evidence; and (b) the kinetic profiles of individual steps in a cycle should, wherever possible, be studied independently from the global kinetics of the cycle.

These two lessons make it evident that kinetics figure prominently in mechanistic analysis of catalytic reactions. In that same review, however, Halpern noted that a widespread limitation of mechanistic research at that time was the preponderance of structural and spectroscopic studies that failed to relate their findings to the kinetics of the catalytic reaction cycle (termed "global" or "phenomenological" kinetics for the remainder of this review). Twenty-five years later, this remains an apt comment. Despite the tremendously increased accuracy of experimental kinetic measurements, despite a proliferation of in situ tools that allow us to look inside a catalytic cycle while the reaction is proceeding, and despite the increased facility of data manipulation methods, global kinetic analysis on catalytic networks is largely carried out the way we did at the beginning of the last century. In particular, catalytic kinetic studies under conditions where two substrate concentrations change simultaneously remain rare. Kinetic measurements of the global catalytic cycle are often seen as the tedious and arduous step taken only after the rather more exciting structural and spectroscopic work has illuminated the mechanistic fine

[†] Department of Chemistry.
[‡] Permanent address: Mitsubishi Pharma Corp., Kamisu, Ibaraki 314-0255, Japan.
[§] Department of Chemical Engineering and Chemical Technology.

10.1021/jo052409i CCC: $33.50
Published on Web 06/16/2006

points; thus, the global kinetic analysis of the catalytic cycle is asked only to confirm what has already been proposed.

This Perspective illustrates how the methodology of reaction progress kinetic analysis can turn this conventional approach around: we advocate doing the global catalytic reaction kinetics *first*, not last! Reaction progress kinetic analysis[3] can provide a rapid and comprehensive understanding of the concentration driving forces operating on a steady-state catalytic cycle at the outset rather than at the end of a mechanistic investigation, in a fraction of the time and number of experiments that would be required in a classical kinetic approach. Acquiring this information even before a reaction mechanism is proposed can limit the number of plausible reaction pathways under consideration and can inform the experimental direction of other mechanistic tools we might employ. For example, this kinetic knowledge can give clues about what species might and might not be isolable and which stoichiometric steps might and might not be feasible to study independently.

A number of examples of Pd-catalyzed aryl halide coupling reactions will serve to demonstrate how reaction progress kinetic analysis provides a kinetically informed approach to mechanistic study. A tremendous body of synthetic and mechanistic work has been assembled for these reactions,[4−8] offering pertinent illustrations of the Halpern admonitions noted above. Some of these reaction networks have been characterized by a "homeopathic"[9] concentration of active Pd within the cycle, with large reservoirs of spectator Pd species identifiable and in some cases isolable.[10] Several reaction systems within this class have lent themselves to careful stoichiometric study of individual steps,[11] providing valuable information about the catalytic reaction network.

Before discussing how our kinetic analysis helps to inform the mechanistic investigations of several Pd-catalyzed aryl halide coupling reactions, we give a brief introduction to the methodology of reaction progress kinetic analysis and to the in situ kinetic measurement tools we employ.

A Graphical Approach to Reaction Progress Kinetics

We define reaction progress kinetic analysis as the **analysis of experimental data acquired over the course of a reaction under synthetically relevant (non-pseudo zero order) substrate concentrations.** Typically, this involves reactions where the concentrations of two or more substrates decrease simultaneously over the course of the reaction. Analysis of reaction progress data may be carried out at several different levels. In its most comprehensive form, reaction progress kinetic analysis employs detailed kinetic modeling involving numerical integration of the differential equations describing the rates of elementary steps in a proposed reaction network. Such methodology may be employed using data from any experimental technique that can deliver an accurate measure of how concentrations change as a function of reaction progress. Methods using differential changes in concentration with time date back to the time of van't Hoff[12] even if they are less commonly employed than methods that use concentration data directly.

The methodology of reaction progress kinetic analysis to be described in this Perspective offers a graphical approach requiring less mathematical prowess than that described above. Because organic chemists have been slow to embrace such kinetic modeling tools, classical graphical approaches to catalytic kinetic analysis dating back to the early 20th century[13−15] remain popular mechanistic tools today.[16] These methods focus on linearizing the rate equation for simple catalytic networks in order to extract kinetic parameters from the slope and intercepts. Reactions involving two different substrate concentrations are problematic, however, because a separate linear plot must be constructed for each substrate in turn while holding the other concentrations constant. This is where our graphical approach offers a key advantage: rapid extraction of kinetic information may be accomplished in a minimum number of carefully designed experiments where two substrate concentrations are changing at once. As will be described, this methodology relies on constructing plots of various functions involving reaction rate vs substrate concentration, which we term "graphical rate equations". While this methodology may be considered a subset of the field of differential kinetics, what we offer differs from differential methods as taught[17] and practiced[18] today; it aims to appeal to chemists preferring a visual, graphical, approach to global kinetics, while making use of the wealth of information contained in the voluminous data sets readily obtained by accurate in-situ monitoring of reaction progress.

Reaction Calorimetry as a Kinetic Tool

Mechanistic studies by our group focus on detailed reaction progress kinetic analysis using in situ tools that provide a virtually continuous temporal reaction rate profile. Our experimental technique of choice in many cases is reaction calorimetry. This technique has a long history as a mechanistic and development tool in a number of areas of industrial chemistry[19−23] including biocatalysis, polymerization, and pharmaceuticals. Consider a catalytic reaction proceeding in the absence of side reactions or other thermal effects. The energy characteristic of the transformation—the heat of reaction, ΔH_{rxn}—is manifested each time a substrate molecule is converted to a product molecule. This thermodynamic state function serves as the proportionality constant between the heat flow, q, and the reaction rate (eq 1).[24] When the reaction under study is the predominant source of heat flow, the fractional heat evolution at any point in time is identical to the fraction conversion of the limiting substrate (eq 2). Fraction conversion is then related to the concentration of the limiting substrate via eq 3. First and foremost in any kinetic study using reaction calorimetry, we must confirm the validity of the method for the system under study by showing that eq 2 holds. Comparing the temporal fraction conversion obtained from the heat flow measurement with that measured by an independently verified measurement technique, such as chromatographic sample analysis or FTIR or NMR spectroscopy, confirms the use of the calorimetric method.

$$q = \Delta H_{rxn} \cdot \begin{pmatrix}\text{reaction}\\ \text{volume}\end{pmatrix} \cdot \text{rate} \tag{1}$$

$$\text{fraction conversion} = f = f_{final} \cdot \frac{\int_0^t q(t)\mathrm{d}t}{\int_0^{t(\text{final})} q(t)\mathrm{d}t} \tag{2}$$

$$[\text{substrate}] = [\text{substrate}]_0 \cdot (1 - f) \tag{3}$$

The above analysis may be extended to more complex systems with multiple reactions according to eq 4 for a system of j reactions under study:

$$q = \begin{pmatrix}\text{reaction}\\ \text{volume}\end{pmatrix} \cdot \sum_j \Delta H_{rxn,j} \cdot (\text{rate})_j \tag{4}$$

SCHEME 1

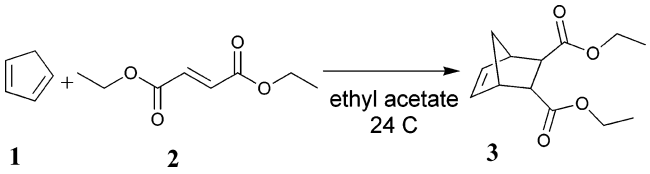

Reaction calorimetry has been used to study both parallel and consecutive reaction pathways.[25−27] Information about temporal product profiles from an independent technique and/or calculations of theoretical heats of reaction are used to partition the heat flow appropriately between the different reactions, and kinetic modeling methods may be applied to the data to assess proposed reaction networks.

It must be noted that the graphical methodology to be described in this Perspective can treat multiple reactions only if the system exhibits time-independent stoichiometry. This same caveat applies equally to classical linearization techniques such as the Lineweaver−Burk or other reciprocal plots. Detailed kinetic modeling approaches using reaction progress data collected via reaction calorimetry or other techniques do not suffer from this constraint.

It is also important to note that many commercial reaction calorimeters are not suitable for monitoring reactions that are very fast (less than ca. 5 min) or very slow (longer than ca. 8 h). In the former case, accounting for the time lag of heat flow through the reactor walls can become inaccurate; in the latter case, the signal becomes too low to provide accurate measurement of rate.

We may illustrate the use of reaction calorimetry with the simple example shown in Scheme 1, a textbook case of an uncatalyzed Diels−Alder transformation. Reaction rate obtained from monitoring the heat flow of this reaction is plotted as a function of time in Figure 1a.[28] These data may be converted to fraction conversion vs time using eq 2, as shown in Figure 1b. In Figure 1b we also compare the reaction calorimetry conversion profile to that obtained from ^{1}H NMR spectroscopic monitoring of the reaction. The close agreement between the two techniques confirms that reaction calorimetry provides a valid measure of reaction progress.

Figure 1 illustrates another key advantage of reaction calorimetry as a kinetic tool. With this method, rate is obtained directly without the need to differentiate a concentration profile, as must be done in order to convert NMR data to reaction rate. The issue of converting concentration data to rate has been discussed previously.[18] In Figure 1a, the blue circles show that considerable scatter may result when the rate is determined from the NMR concentration profile, and smoothing functions are often applied.

As we will see in the next sections, the graphical manipulations we develop in the methodology of reaction progress kinetic analysis presented here rely on a *highly accurate, virtually continuous account of the relationship between reaction rate and substrate concentration*. The enhanced accuracy as well as increased data density (20 data points per minute in Figure 1) offered by reaction calorimetric monitoring make this our method of choice, wherever possible, for this type of kinetic analysis. As is revealed by the examples presented here as well as in the references cited, a wide range of catalytic systems is amenable to this experimental protocol.

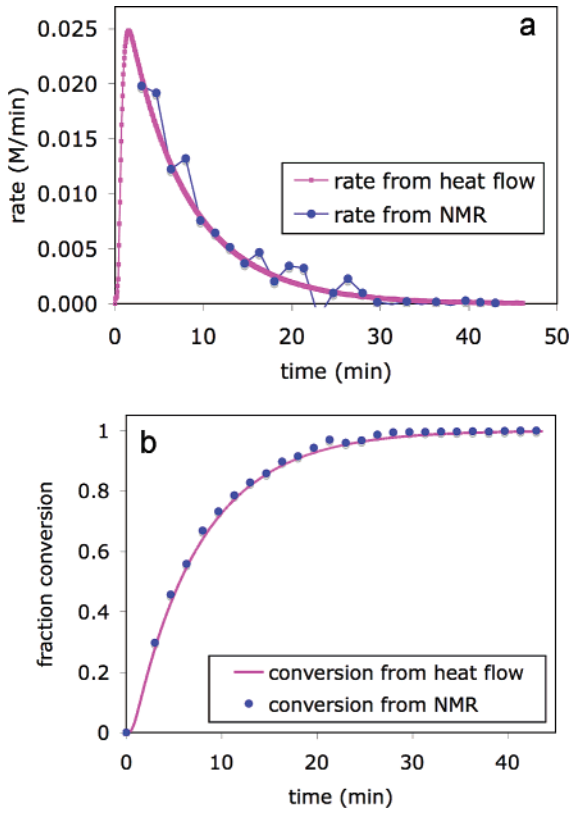

FIGURE 1. Reaction progress profile for the reaction in Scheme 1 obtained using reaction calorimetry and ^{1}H NMR spectroscopy. (a) Reaction rate vs time. NMR spectroscopic data are converted from conversion to rate by differentiation. (b) Fraction conversion vs time. Rate data from heat flow are converted to conversion via eq 2.

Reaction Progress Kinetic Analysis: Introductory Examples

Classical kinetic studies of a reaction such as that shown in Scheme 1 are typically carried out under conditions where the concentration of one of the substrates is fixed while the rate dependence of the other substrate's concentration is probed. This is accomplished either by using initial rate measurements, where neither substrate's concentration changes significantly in a given experiment, or by employing pseudo-zero-order conditions, where only one substrate's concentration changes. These procedures require a large number of repetitive experiments to produce data sufficient to provide a record of reaction rate over a range of concentrations of both substrates.

Reaction progress kinetic analysis allows extraction of the same kinetic information with significantly fewer experiments. The key to this analysis lies in making use of the reaction stoichiometry. For the simple Diels−Alder reaction of Scheme 1, a mass balance tells us that for each molecule of diene **1** consumed, one molecule of dienophile **2** is also consumed. This relationship is quantified in eq 5. The parameter of interest for our analysis is the *difference* between the initial concentrations of the two substrates. This parameter is a constant in any given experiment, and we call it the excess, or [*e*], with units of molarity (eq 6).[29] The quantity [*e*] allows us to relate the two

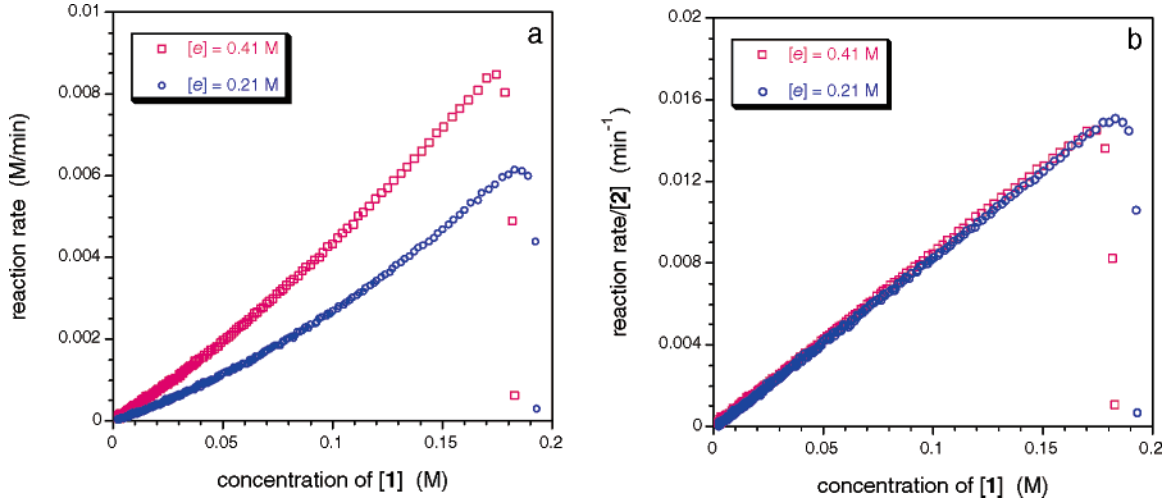

FIGURE 2. Reaction progress profiles from reaction calorimetric monitoring of two reactions of Scheme 1 carried out using different values of excess [*e*]: (a) reaction rate vs [**1**]; (b) reaction rate/[**2**] vs [**1**].

substrates' concentrations at any point during the reaction (eq 7).

$$[\mathbf{2}]_0 - [\mathbf{2}] = [\mathbf{1}]_0 - [\mathbf{1}] \tag{5}$$

$$[e] = [\mathbf{2}]_0 - [\mathbf{1}]_0 \tag{6}$$

$$[\mathbf{2}] = [e] + [\mathbf{1}] \tag{7}$$

The excess [*e*] can be large, small, positive, or negative. When pseudo-zero-order conditions in [**2**] are employed, [*e*] is $\gg$ [**1**]. Under conditions of practical synthetic experiments, [*e*] is usually small, and [**1**] and [**2**] are only slightly different from each other. These synthetically relevant conditions are employed in reaction progress kinetic analysis.

Experimental Protocols

The key to the graphical methodology developed in this Perspective lies in defining two different experimental protocols: (a) "different excess [*e*]" experiments and (b) "same excess [*e*]" experiments. We will use the simple Diels−Alder reaction of Scheme 1 to help illustrate how reaction progress data from only *two* separate reactions can determine reaction orders in *both* substrates [**1**] and [**2**]. Then we turn to a catalytic aldol reaction to demonstrate how one further experiment can confirm whether the catalyst concentration remains constant over the course of the reaction.

(a) "Different Excess [*e*]" Experiments. In the case of the uncatalyzed Diels−Alder reaction, we know a priori that this bimolecular elementary reaction exhibits overall second-order kinetics as given by eq 8.

$$\text{rate} = k\cdot[\mathbf{1}]\cdot[\mathbf{2}] \tag{8}$$

Figure 2a plots rate vs [**1**], our simplest "graphical rate equation," for two reactions carried out at different values of the excess [*e*]. Note that in such a plot the direction of reaction progress is from right to left, with substrate being consumed over the course of the reaction. The curvature in the plots shown in Figure 2a reveals the classical difficulty in extracting reaction orders under conditions where two substrate concentrations are changing at the same time. Reaction progress kinetic analysis overcomes this problem with a simple procedure to "normalize" the value of rate at any given time by concentration at that same given time. This is shown in eq 9 for normalization by [**2**], and a similar normalization may be performed on [**1**].

$$\text{normalized rate} = \frac{\text{rate}}{[\mathbf{2}]} = k\cdot[\mathbf{1}] \tag{9}$$

Equation 9 introduces a new "graphical rate equation" plotted in Figure 2b, which now has the function rate/[**2**] on the *y*-axis. As predicted by eq 9, we obtain a straight line with slope = *k*, confirming that the reaction is first order in [**1**].

The order in [**1**] is not the only information available from the data plotted as this normalized function in Figure 2b. The fact that the two curves from two reactions carried out at two different [*e*] values fall on top of another—i.e., they "overlay"—is significant. Looking back at eq 7, we see that any two reactions with different values of [*e*] have *different* concentrations of **2** at any given concentration of **1**. The "overlay" in Figure 2b shows that the function (rate/[**2**]) is not a function of [**2**], which tells us that the reaction exhibits first-order kinetics in the "normalized" substrate [**2**].

Let's summarize the information we obtain from a plot of "normalized rate" vs concentration for two reactions carried out with different values of [*e*] such as in Figure 2b:

- **"Overlay" between the two curves** reveals that the reaction exhibits first-order kinetics in concentration of the "normalized" substrate. Thus, the overlay in Figure 2b confirms that the Diels−Alder reaction exhibits first-order kinetics in [**2**].
- **The shape of the curve** reveals the reaction order in the concentration of the substrate plotted as the *x*-axis variable; for example, the straight line in Figure 2b confirms that the reaction exhibits first-order kinetics in [**1**].

This example demonstrates for a simple case how a reaction rate law may be comprehensively defined in two substrates by just *two* reaction progress experiments employing two *different* values of excess [*e*]. A classical kinetics approach involving initial rate measurements would require perhaps a dozen separate experiments to obtain the same information.

(b) "Same Excess" Experiments. We now describe a second set of experiments that are critical to this methodology when it is carried out on *catalytic* systems. Determining reaction orders

SCHEME 2

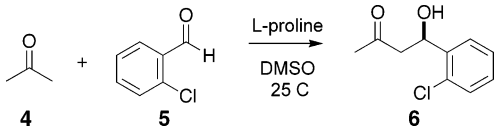

TABLE 1. Comparison of the Initial Conditions of Two Reactions Carried out at the Same Excess [*e*] and Their Concentrations during the Reaction

component	acetone **4**	aldehyde **5**	[*e*]	product **6**
expt 1: initial conditions	2.5 M	0.5 M	2 M	0 M
expt 2: initial conditions	**2.25 M**	**0.25 M**	2 M	0 M
expt 1: 50% conversion	**2.25 M**	**0.25 M**	2 M	0. 25 M

in [substrate] from rate measurements in catalytic reactions implicitly requires that the active catalyst concentration remains unchanged during the kinetic measurement. Catalyst activation and deactivation are common phenomena that can change the active catalyst concentration. A quandary in conventional kinetic analysis is how to be certain that such effects do not complicate the kinetic analysis under any given set of reaction conditions. Initial rate methods are often employed in the hope of avoiding the need to address the problem of catalyst deactivation; however, initial rates can be problematic for kinetic analysis in cases where induction behavior of a precatalyst is observed. Extensive spectroscopic studies are sometimes carried out to observe changes in the concentration of catalytic intermediates, but a case must be made to show that such experiments do in fact probe *active* catalyst species.

Reaction progress kinetic analysis offers a reliable alternative method to assess the stability of the active catalyst concentration, again based on our concept of excess [*e*]. In contrast to our "different excess" experiments described above, now we carry out a set of two experiments at the *same* value of excess [*e*]. We use the proline-mediated aldol reaction shown in Scheme 2 as our illustrative example. Oxazolidinone formation between proline and aldehydes or ketones has been observed,[30] and this reaction can effectively decrease the active catalyst concentration. It has recently been shown that the addition of water can suppress this catalyst deactivation.[31] Here, we describe how two reaction progress experiments carried out at the same excess [*e*] can be used to confirm the deactivation of proline in the absence of added water as well to demonstrate that proline concentration remains constant when water is present.

The proline-mediated aldol reaction in Scheme 2 was carried out under the two sets of conditions shown in Table 1,[32] employing the same catalyst concentration but different initial concentrations of the two reactants. These initial concentrations are chosen such that the value of the excess, [*e*], is the same in the two experiments, although more conventionally reported parameters—for example, the number of equivalents of acetone and the catalyst mol %—differ between the two experiments. What is the significance of this choice of conditions? Table 1 shows that the initial conditions of Experiment 2 are identical to the concentrations of reactants found in Experiment 1 at the point when it reaches 50% conversion (Table 1, bold entries). In fact, from this point onward the two experiments exhibit identical [acetone] at any given [aldehyde] throughout the course of both reactions. This "same [*e*]" experimental protocol leads to another form of graphical "overlay" plot that yields valuable kinetic information: if the two experiments described in Table 1 are plotted together as reaction rate vs [aldehyde], the two curves will fall on top of one another ("overlay") over the range of [aldehyde] common to both *only* if the rate is not significantly influenced by changes in the overall catalyst concentration within the cycle, including catalyst activation, deactivation, or product inhibition. Such plots are shown for the case of the reaction in Scheme 2 in the absence of water and in the presence of water in Figure 3a and b, respectively.[32] The plots do not overlay in the absence of water, but they do when water is present. The "overlay" in these "same [*e*]" experiments in Figure 3b means that the total concentration of active catalyst within the cycle is constant and is the same in the two experiments where water is present. Once conditions for obtaining constant catalyst concentration during reactions are found, we may proceed in probing substrate concentration dependences with confidence that the complicating influence of a changing active catalyst concentration is absent.

Now that we have established the protocol of "same excess" and "different excess" experiments to probe for reaction orders and for catalyst stability, we turn to several examples of Pd-catalyzed ArX coupling reactions to illustrate the power of this methodology to treat the complex rate behavior characteristic of catalytic reactions. We use the same graphical approach developed in the first part of this Perspective, designing a total of three experiments for each of the four Case Studies presented in Schemes 3−6.

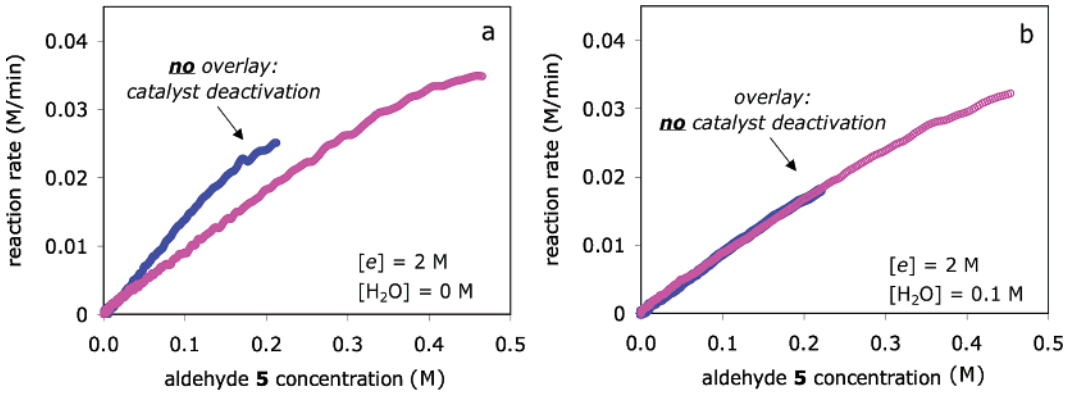

FIGURE 3. Comparison of rate vs [aldehyde] **5** for two reactions of Scheme 2 carried out at the same excess [*e*] with initial conditions as given in Table 1 (magenta dots, experiment 1; blue dots, experiment 2): (a) no water added; (b) 0.1 M water added to the reaction.

SCHEME 3. Case I: Heck Coupling Catalyzed by Pd(P(*t*-Bu)$_3$)$_2$[33]

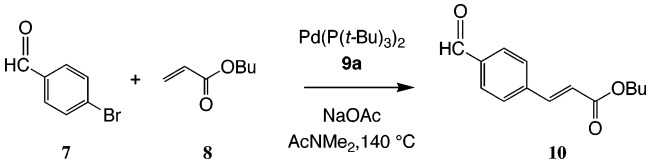

SCHEME 4. Case II: Heck Coupling Catalyzed by Dimeric C−N Palladacycles[34]

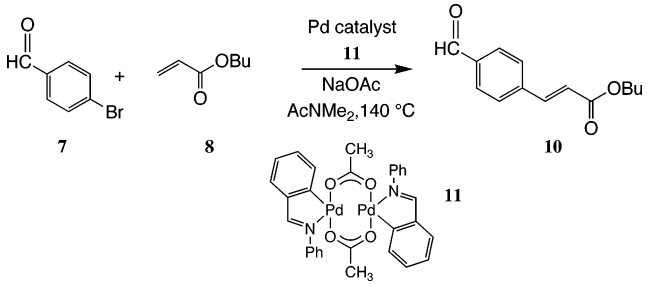

SCHEME 5. Case III: Sonogashira Coupling Catalyzed by in Situ Prepared Pd(P(*t*-Bu)$_3$)$_2$[35]

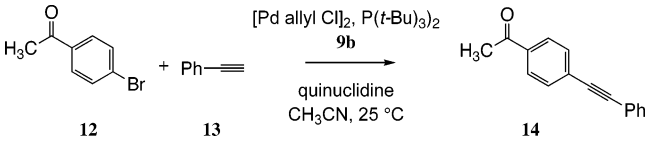

SCHEME 6. Case IV: Amination Catalyzed by Pd/binap[36]

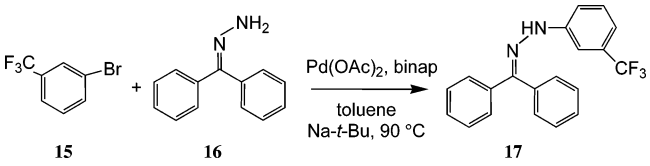

Pd-Catalyzed ArX Coupling Reactions: Four Case Studies

Reaction progress data have been obtained by reaction calorimetric monitoring of the four different reactions shown in Schemes 3−6. These examples include a Heck reaction catalyzed by two different Pd complexes, a Sonogashira reaction, and a Buchwald/Hartwig amination reaction. Reaction calorimetry as a valid measure of rate was verified for each case by comparing conversion obtained from heat flow (eq 2) to that obtained by sampling and GC analysis. This is illustrated in Figure 4.

In each reaction, we designate the aryl halide concentration as [ArX] and we give the second substrate (alkene, alkyne, or amine) the designation [Nu]. We will now see how our set of three experiments, two "same excess" and one further "different excess" experiment, allow us to characterize the global catalytic kinetics of each cycle even before considering possible mechanisms for these reactions.

Reaction Progress Kinetic Analysis of Cases I−IV

Parts a−d of Figure 5 show kinetic data from reaction calorimetric monitoring of each of the four reactions of Cases I−IV shown in Schemes 3−6. In each case, profiles from three reactions are shown: two reactions carried out at the same excess, and one reaction is carried out at a different excess value [*e*]. This set of three experiments defines our kinetic analysis

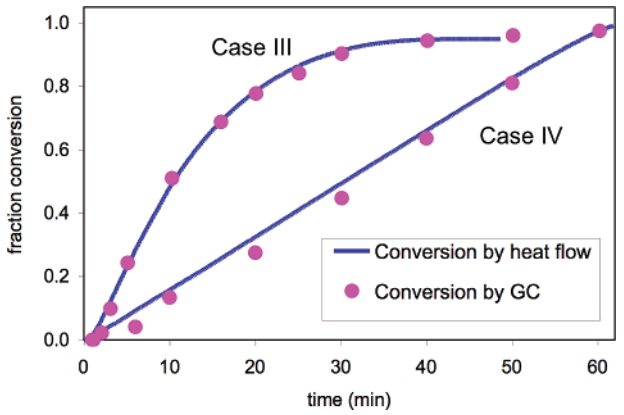

FIGURE 4. Conversion vs time measured by reaction calorimetry (eq 2, solid blue lines) and by GC analysis of samples extracted over time (magenta circles) for the reactions of Case III and Case IV shown in Schemes 5 and 6, respectively.

by combining the requirement to check for catalyst stability (same [*e*] experiments) with the requirement for determining reaction order in [ArX] and [Nu] (different [*e*] experiments).

Simple examination of the concentration profiles in Figure 5 sheds little light on concentration dependences in [ArX] and [Nu] in most of these cases. The capability of our methodology to unravel the information hidden in these data is revealed as we replot them in the form of one of the three "graphical rate equations", eqs 10a−c. The first equation gives a simple plot of rate vs concentration, while the next two present rate "normalized" by one substrate's concentration plotted against the other substrate's concentration. Our task is to seek "overlay" in each of Cases I−IV between data points in the three experiments using one of these graphical rate equations.

$$\text{rate vs [ArX]} \tag{10a}$$

$$\text{rate/[ArX] vs [Nu]} \tag{10b}$$

$$\text{rate/[Nu] vs [ArX]} \tag{10c}$$

In plotting the data from reaction progress measurements in the form of these graphical rate equations, we typically consider the data from ca. 20−80% conversion, leaving out the beginning and end of the reaction. Many reactions exhibit induction periods at the outset and at high conversions we find that normalization by the limiting substrate becomes inaccurate as its concentration approaches zero.

Parts a−d of Figure 6 show "overlay" plots for the reactions of Cases I−IV. Next, we describe what these plots teach us about the concentration dependence of rate on [ArX] and [Nu] in each of the Cases I−IV, followed by a discussion of possible mechanistic implications of these kinetic conclusions.

Case I. Pd(P(*t*-Bu)$_3$)$_2$-Catalyzed Heck Coupling of Butyl Acrylate with 4-Bromobenzaldehyde. Figure 6a shows that plots of rate/[ArX] vs [Nu] (eq 10b) give curves that overlay as horizontal lines. This reveals that the catalyst concentration is stable and that the reaction is

- first order in [ArX]
- zero order in [Nu]

to give the global rate expression

$$\text{rate} \propto [\text{ArX}] \tag{11}$$

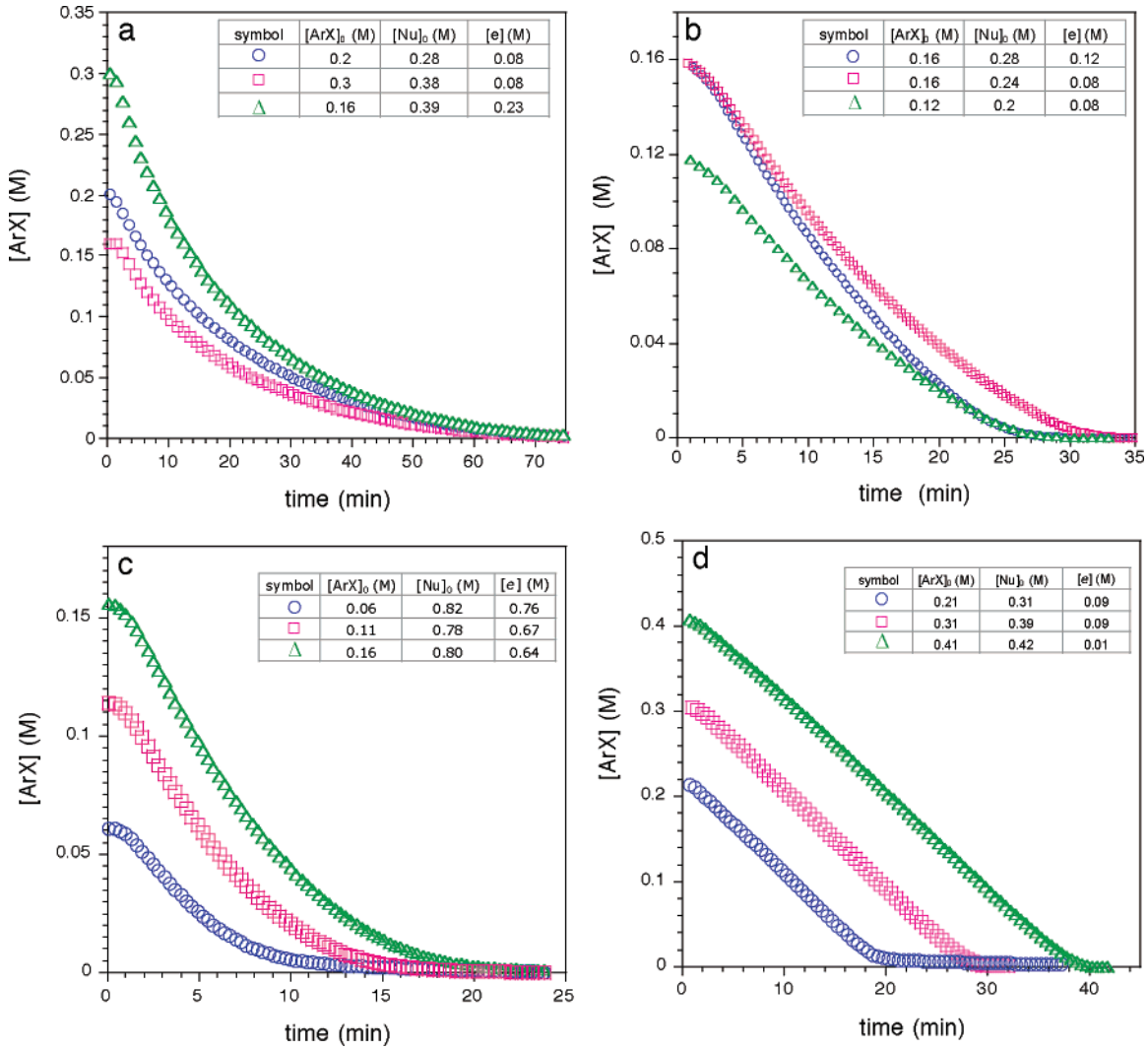

FIGURE 5. Plots of concentration vs time in the four ArX coupling reactions shown in Schemes 3−6. Plots derived from reaction calorimetry data using eqs 1−3. In each case, two reactions have been carried out under conditions of identical excess and one at a different excess as detailed in the figures: (a) reaction of Scheme 3; (b) reaction of Scheme 4; (c) reaction of Scheme 5; (d) reaction of Scheme 6.

Case II. Palladacycle-Catalyzed Heck Coupling of Butyl Acrylate with 4-Bromobenzaldehyde. Figure 6b shows that plots of rate/[Nu] vs [ArX] (eq 10c) give curves that overlay as horizontal lines. This reveals that the catalyst concentration is stable and that the reaction is

- first order in [Nu]
- zero order in [ArX]

to give the global rate expression

$$\text{rate} \propto [\text{Nu}] \tag{12}$$

Note that these orders in substrate in Case II are opposite those found in Case I for the same reaction catalyzed by a different Pd catalyst.

Case III. Pd(P(*t*-Bu)$_3$)$_2$-Catalyzed Sonogashira Coupling of Phenylacetylene with 4-Bromoacetophenone. Figure 6c shows that plots of rate/[Nu] vs [ArX] (eq 10c) give curves that overlay but do not exhibit straight lines. This reveals that the catalyst concentration is stable and that the reaction is

- first order in [Nu]
- complex order in [ArX]

The shape of the profile in this case is indicative of saturation kinetics in [ArX], as in the Michaelis−Menten form given by eq 13. This may be inverted to give the equation in "double reciprocal form" (eq 14). In both equations, V_{max} is the maximum value of the rate function (rate/[Nu]) and K_M is the Michaelis constant, which is related in an inverse fashion to the degree of interaction between ArX and catalyst. As shown in Figure 7, plotting the reciprocal form in eq 14 gives a straight line from which a Michaelis constant K_M of ca. 0.04 M may be derived.

$$\frac{\text{rate}}{[\text{Nu}]} = \frac{V_{max}[\text{ArX}]}{K_M + [\text{ArX}]} \tag{13}$$

$$\left(\frac{\text{rate}}{[\text{Nu}]}\right)^{-1} = \frac{K_M}{V_{max}} \cdot \frac{1}{[\text{ArX}]} + \frac{1}{V_{max}} \tag{14}$$

Case IV. Pd/(binap)-Catalyzed Amination of 3-Trifluoromethylbromobenzene. Figure 6d shows that plots of rate vs [ArX] (eq 10a) give curves that overlay as horizontal lines. This reveals that the catalyst concentration is stable and that the reaction is

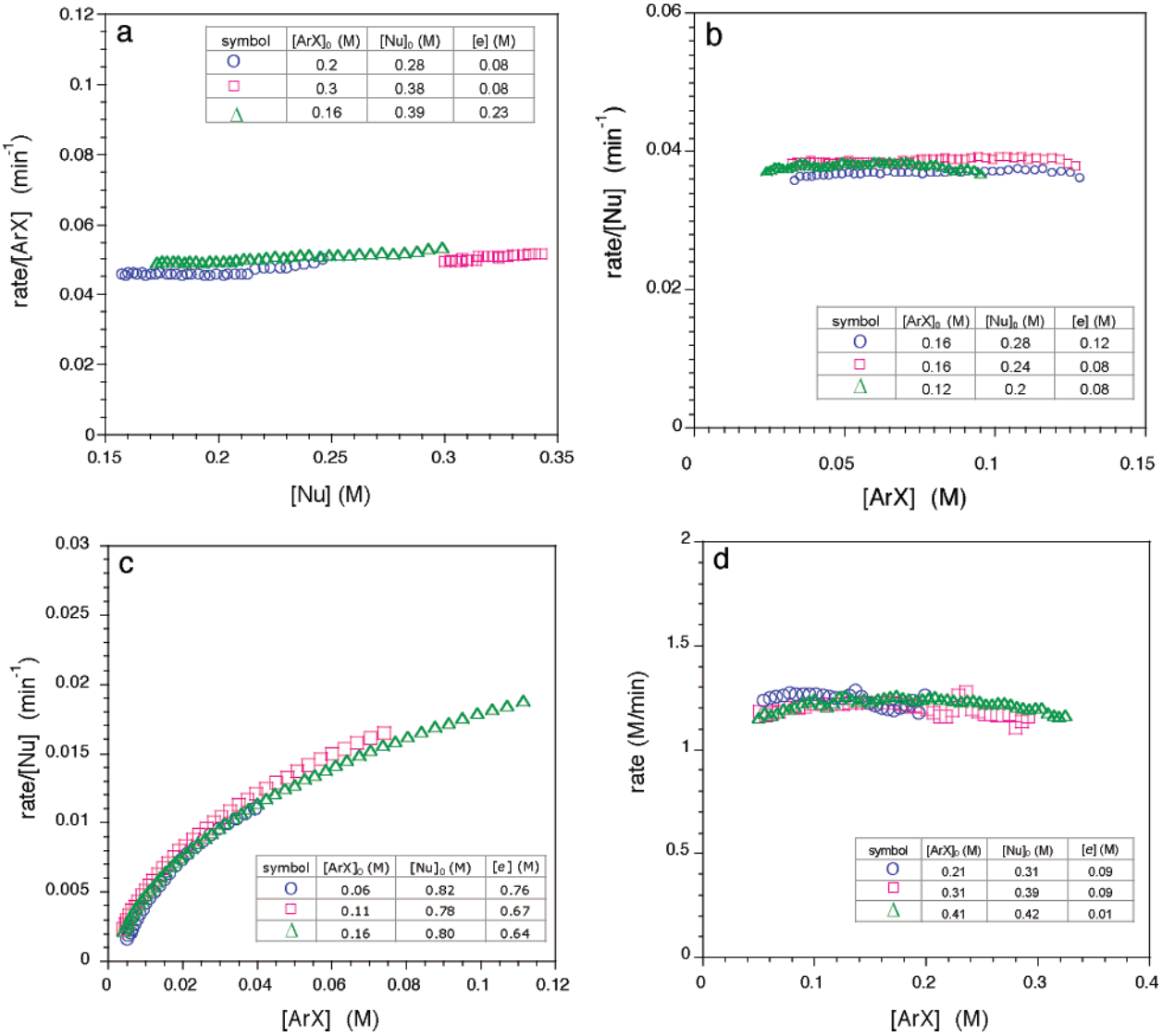

FIGURE 6. Plots of graphical rate equations for the four ArX coupling reactions shown in Schemes 3−6 derived from reaction calorimetry data shown in Figure 5. In each case, two reactions have been carried out under conditions of identical excess and one at a different excess as detailed in the figures: (a) reaction of Scheme 3, data from Figure 5a, graphical rate eq 10b; (b) reaction of Scheme 4, data from Figure 5b, graphical rate eq 10c; (c) reaction of Scheme 5, data from Figure 5c, graphical rate eq 10c; (d) reaction of Scheme 6, data from Figure 5d, graphical rate eq 10a.

- zero order in [ArX]
- zero order in [Nu]

to give the global rate expression

$$\text{rate} = \text{constant} \qquad (15)$$

Overlay Plots: The Details

A question that often arises in discussions of reaction progress kinetic analysis plots such as Figure 6a−d is the following: How do we know which of the "graphical rate equations" of eqs 10a−c to use in any given case? The answer is that, a priori, we do not know! We simply try each one in turn until we find a relationship that exhibits "overlay". Consider Cases I and II. Figure 8 reveals what we would have found if we had tried eq 10c instead of eq 10b for Case I and if we had tried eq 10b instead of eq 10c for Case II. We see that in each case the two "same [*e*]" experiments still exhibit overlay; this is expected, because confirmation of catalyst stability is independent of how we plot the data. However, the "different [*e*]" experiments for these two cases no longer exhibit overlay when we choose these graphical rate equations instead of those we used in Figure 6. This lack of overlay tells us that the reaction rate law does *not* follow the relationship suggested by the form of equation we have plotted, i.e., the reaction does *not* exhibit first-order kinetics in concentration of the normalized substrate. In some examples, we may find that curves of different [*e*] do not overlay no matter which graphical rate equation we choose; that result would suggest that the reaction exhibits complex orders in both substrates.

Another question that arises concerning overlay plots is: how good does the overlay need to be? This may be answered rigorously with a statistical examination of the data that can give tolerances on the reaction orders obtained; we may find that a reaction exhibits first-order kinetics ± 5%, for example. Typically, however, we find that what appears by eye to be a reasonable overlay will give a good enough estimate of reaction order for us to make use of in our subsequent mechanistic investigations.

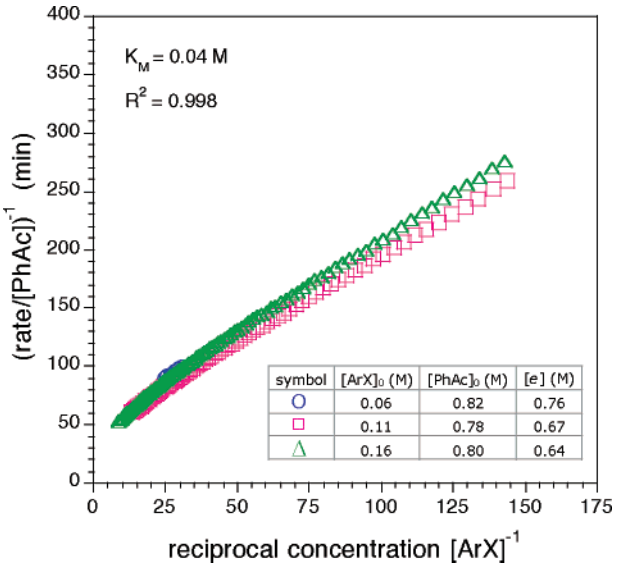

FIGURE 7. Data from Figure 6c replotted in double-reciprocal form.

It is also important to keep in mind that the reaction orders obtained via these overlay plots are strictly valid only over the range of concentrations under which the plots were made, and extrapolation of the findings to concentrations outside this range should be made with caution. This message is equally important for kinetic investigations carried out by classical methods, especially under pseudo-zero-order conditions. For example, stoichiometric studies of the oxidative addition of ArX to Pd complexes in the presence of phenylacetylene **13** (similar to the Sonogashira reaction of Case III) showed the rate to be suppressed by increasing concentrations of **13**.[37] This was suggested to be due to competitive coordination of the terminal alkyne to Pd. However, those studies were carried out under conditions where 50−200 equiv of **13** were employed compared to the aryl halide, possibly accentuating the level of competition beyond what might be found under synthetically realistic conditions. Similarly, a recent study of stoichiometric oxidative addition of ArX to Pd(binap)$_2$ showed a small dependence of the rate on the presence of amine,[38] in contrast to earlier work by the same group where the rate was independent of [amine].[39,40] The discrepancy was rationalized by the fact that amine concentrations in the earlier studies had been too low to detect the dependence. Thus, studies carried out at either anomalously high or anomalously low concentrations can lead to misleading results for reaction orders in substrate concentration. This highlights a particular advantage of reaction progress kinetic analysis: because we employ reactant concentrations in a range similar to those used in synthetic experiments, we can be assured that the kinetic information we derive will be relevant to the practical reaction carried out under these conditions. As has been pointed out previously,[41] the pseudo-zero-order conditions of classical kinetic experiments must be interpreted with the caveat that the distorted concentration conditions may alter the observed kinetics.

Mechanistic Implications Derived from the Kinetic Plots

The reaction orders in substrate concentration for the examples of Cases I−IV have been obtained by carrying out just three experiments in each of these four cases. Streamlining the acquisition of kinetic information even before proposing a reaction mechanism allows us to limit our consideration to mechanisms we know to be consistent with the observed kinetics. In any case, it is important to emphasize that proposed mechanisms are necessarily only hypotheses; we may disprove a mechanism with experimental evidence but we cannot claim to prove it because alternate scenarios may be found that are also consistent with the data.

For these four examples, one general mechanism that may be shown to be consistent with the data in all cases involves the oxidative addition of ArX to an active Pd species as the first step in the cycle, followed by addition of either the alkene, alkyne, or amine as Nu. With this hypothesis, the differences in the reaction orders in substrate for the four cases may be rationalized by a shift in the rate-limiting step and catalyst resting state from one case to another.

Simplified[42] catalytic cycles based on this mechanistic hypothesis are given in Scheme 7 and are described below. These proposals are presented as possible scenarios consistent with the kinetics we observe, to facilitate other experimental mechanistic probing for further support or refutation.

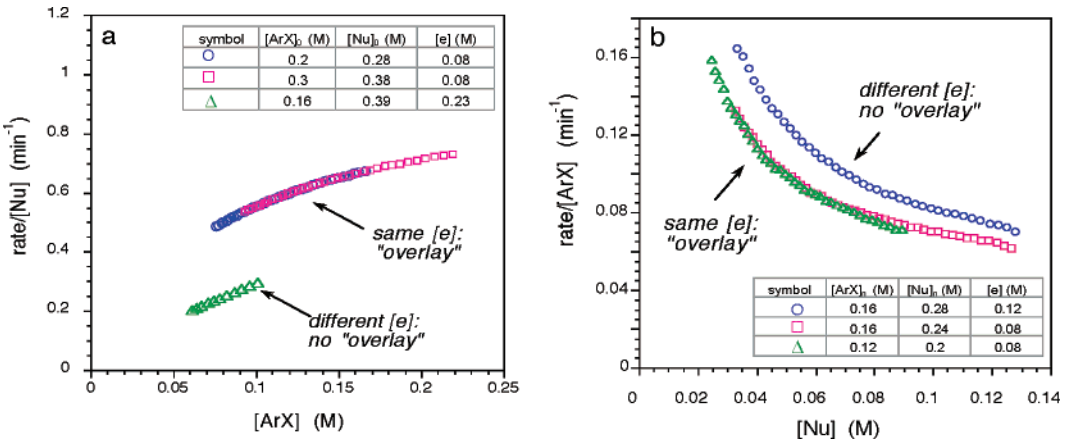

FIGURE 8. Alternative graphical rate equations for the examples shown in Schemes 3 and 4. The rate function plotted on the *y*-axis in each case results in overlay for the same [*e*] experiments but not for the experiments carried out at different [*e*], indicating in each case that the reaction does *not* exhibit first-order kinetics in the normalized substrate concentration: (a) reaction in Scheme 3 and Figure 5a; (b) data from reaction in Scheme 4 and Figure 5b.

SCHEME 7. Proposed Mechanisms for the Reaction Examples of Schemes 3−6 Based on the Kinetic Analysis Shown in Figures 5 and 6[a]

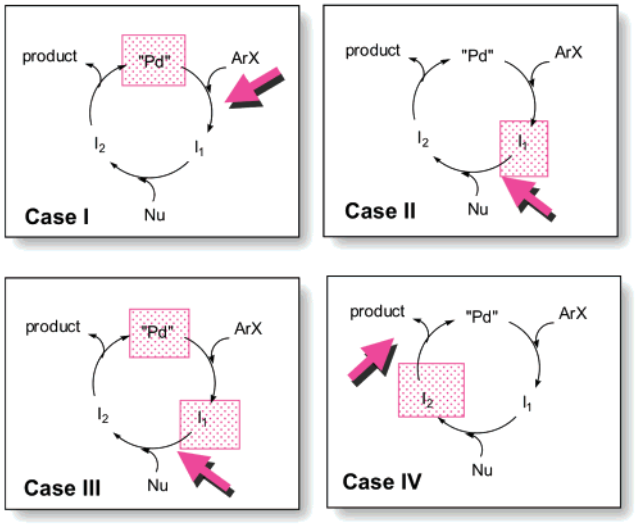

[a] Proposed rate-limiting step and catalyst resting states are highlighted by arrows and shaded rectangles, respectively.

• In Case I, oxidative addition is proposed as the rate-limiting step. The resting state for catalyst within the cycle under this proposal would be the "Pd" species at the entry point to the cycle.

• Case II is consistent with addition of the nucleophile to the oxidative addition complex as rate-limiting. The observed zero order in [ArX] is consistent with the mechanism in Scheme 7 if the oxidative addition complex species I_1 is fully saturated, suggesting that I_1 is the resting state within the cycle.

• Reaction of Nu with the oxidative addition complex may be proposed as rate-limiting in Case III, and saturation kinetics may be invoked as in Case II, but here the curvature in the graphical rate equation plots of Figure 6c suggests that species I_1 is not fully saturated. These data are consistent with the mechanism in Scheme 7 with the catalyst within the cycle partitioned between the "Pd" species and the oxidative addition complex I_1, giving a complex order in [ArX].

• Zero-order behavior in both substrates as observed in Case IV implies that a step occurring after the addition of both substrates is rate-limiting and that the resting state may be a species I_2 containing Nu added to the oxidative addition complex I_1.

Note that these mechanistic proposals make no attempt to define the structure of the "Pd" species that serves as the entry point to the cycle or the nature of intermediates I_1 or I_2 in each case; it is important to emphasize that the proposals in Scheme 7 are as far as our kinetic data can take us. Consider, however, the wealth of information we have already been able to extract about these four examples from only three reaction experiments in each case and where this information may take us. First, we can be certain that catalyst deactivation is not a factor in any of these reactions; second, we can learn how strongly the reaction rate depends on each substrate; third, we can propose where the "bottlenecks" in the cycle are; indeed, for a given proposed mechanism, we can estimate the relative populations of proposed intermediates even before we have acquired any information about what these species look like! Designing further experiments aimed at excluding possible mechanisms becomes much easier when we know at the outset from the global kinetics what a proposed mechanism requires.

Simple examination of the three kinetic profiles of [ArX] vs time plotted in Figure 5a−d was not sufficient to get us there, however; the information contained within these data becomes clear only by manipulation via the "graphical rate equations" of eqs 10a−c. The "overlay" we observe in the plots in Figure 6 represents a kind of "pattern-recognition" that clues us in to particular relationships between rate and concentration defined in each case by the particular graphical rate equation we chose to plot.

Probing the Nature of the Catalytic Intermediates

The nature of the intermediates we propose in each case in Scheme 7 must be probed by drawing upon mechanistic tools other than global kinetic analysis. We can, however, use our kinetically streamlined picture to give us clues about where to begin further mechanistic analysis. For example, we might study the stoichiometric oxidative addition of ArX to the Pd catalyst in Case I. Our mechanistic proposal suggests that the rate of this stoichiometric reaction should equal that of the catalytic reaction. Spectroscopic studies (e.g., ^{31}P NMR) might help to define the nature of the "Pd" species that is suggested to be the resting state. Reaction of the isolated oxidative addition complex in this case, however, may not provide a meaningful comparison with catalytic data.[43] In Cases II and III, formation and isolation of oxidative addition complexes might allow study of their rate of decay as reactants in the stoichiometric addition of nucleophile, which could then be compared to the catalytic reaction rates. In Case IV, the stoichiometric oxidative addition should proceed faster than the rate measured for the catalytic cycle. The nature of the Pd species I_2 containing both ArX and Nu in this case might be accessible with spectroscopic studies. If an isolable species is found, the rate of the stoichiometric reaction of this species with base could be compared to the catalytic reaction rate.

While such mechanistic experiments are not the focus of this review, full mechanistic investigations of these examples will be reported separately.

The key point to keep in mind when planning experiments for further mechanistic analysis is this: once the global kinetics have been defined, the burden of proof lies with all other mechanistic tools to demonstrate consistency with what we have learned from these phenomenological catalytic kinetics. Obtaining this kinetic information at the outset of our investigation may eliminate unproductive mechanistic detours that might focus on species demonstrated by the kinetics to be unrelated to the catalytic cycle.

This point is underscored by two recent examples where reaction progress kinetic analysis of the global kinetics of the catalytic cycle has demonstrated that previously proposed mechanisms are incorrect.[39,44,45] Both examples involve the amination of ArX catalyzed by Pd/binap in reactions similar to our Case IV. In one case,[44] ArX addition to an amine-bound species was proposed to explain an apparent positive order dependence on [secondary amine] that was ultimately found to be due to catalyst deactivation.[45] An important lesson may be learned from this example: while the "same [*e*]" experiments described here to test for catalyst deactivation were not reported in that study, such experiments could have been used to discount that mechanistic proposal from the outset. In the second

SCHEME 8. Examples of "Off-Cycle" Species and Their Influence on the Resting State of the Catalyst[a]

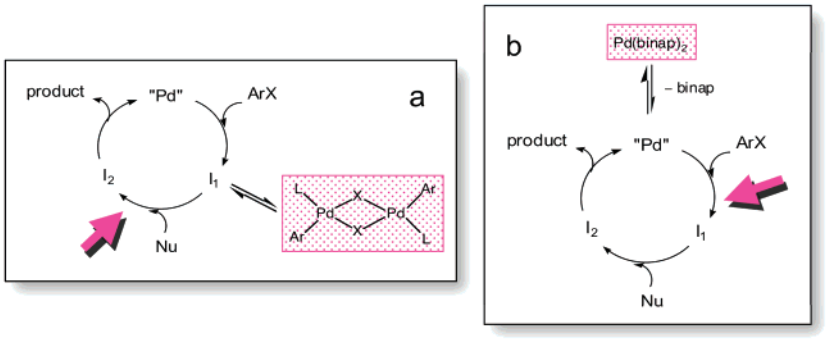

[a] Key: (a) halide-bridged dimer formation in the Heck coupling example of Case II; (b) precatalyst reservoir in the amination reaction of refs 39, 44, and 45.

example, a species proposed to lie on the catalytic cycle was shown instead to lie off the cycle.[45] When such off-cycle species remain in equilibrium with intermediates on the catalytic cycle, they are termed "dead-end" species;[46] this example and another case of an off-cycle species are described in the next section.

Comments Concerning Off-Cycle or "Dead-End" Species

The Heck coupling example of Case II above represents an example where information about the nature of the active intermediates is difficult to obtain directly due to the extremely low concentration of catalytic species within the cycle. The nature of the active Pd^0 species presumably formed from the dimeric palladacycle precursor is not known. However, Br-bridged dimeric palladacycles have been isolated after Heck coupling reactions of ArBr starting from acetate-bridged palladacycle precursors.[10] The reaction has also been shown to exhibit close to half-order kinetics in [Pd].[34,47] These observations help to refine the mechanism proposed for Case II in Scheme 4 as shown in Scheme 8a, where a halide-bridged dimer lies off the cycle in equilibrium with the oxidative addition species I_1. The extremely high activity of the very low concentration of Pd employed (10^{-4} M in Case II[34]) becomes all the more remarkable when we consider that most of the Pd is tied up as the off-cycle dimer. This case provides a good analogy to the Wilkinson's catalyst case, where the reaction proceeds via a minute concentration of a highly active species, with a number of off-cycle species being observed, including those incorporating reactants.

In Pd/binap-catalyzed amination reactions similar to our Case IV, the off-cycle species $Pd(binap)_2$ has been observed by NMR spectroscopy during the reaction.[39] Because this was the only species observed, and because its concentration decreased by no more than 15% over the course of the reaction, this complex was proposed to lie directly on the catalytic cycle. Stoichiometric studies suggested reversible ligand dissociation as the first and rate-limiting step.[39,40,48] An alternate explanation involving slow, off-cycle activation of the $Pd(binap)_2$ was suggested[44,49] and has since been supported by results showing conclusively that the global kinetics are not consistent with $Pd(binap)_2$ being on the cycle.[50] A refined mechanistic proposal with $Pd(binap)_2$ as the resting state lying *off* the cycle is shown in Scheme 7b.

An interesting point in this example is that the reversible off-cycle ligand dissociation step exhibits different kinetics in [ArX] in a stoichiometric oxidative addition sequence than it does in the global catalytic reaction under identical conditions. This is a common feature of "dead-end steps"[46] associated with catalytic cycles. In addition, the stoichiometric oxidative addition of ArX to $Pd(binap)_2$ exhibits a small dependence on amine concentration that is not observed in the catalytic reactions. In a further analogy to the Halpern hydrogenation studies, in this case observed discrepancies between stoichiometric and catalytic kinetics helped to correct an incorrect proposed catalytic reaction mechanism.

Distinguishing between Mechanistic Possibilities

The observed overall zero-order kinetics in the Pd(binap)-catalyzed amination reaction of Case IV is consistent with a rate-limiting step occurring after addition of the amine to the oxidative addition complex (Scheme 6). However, zero-order kinetics would also be observed if $Pd(binap)_2$ lies on the cycle and ligand dissociation is rate-limiting. Catalytic kinetic experiments can be used to distinguish between these two possibilities. We found that the reaction of Case IV proceeds significantly faster and switches to positive order kinetics when *n*-hexylamine is employed as Nu instead of the deactivated hydrazone.[36] Clearly, ligand dissociation cannot be rate-limiting if a change in a subsequent step in the cycle increases the rate. Hence, we may discard the proposal of $Pd(binap)_2$ lying on the cycle as being inconsistent with the data.

Multi-Step Reactions as "Chameleons"

In $Pd(binap)_2$-catalyzed reactions of primary amines with PhBr, the major species is the off-cycle complex $Pd(binap)_2$. In our analogous reaction of Case IV with the *same catalyst* but *different substrates*, we suggested that the catalyst resting state is intermediate I_2 in Scheme 7. Similarly, we saw in the Heck reaction examples of Cases I and II that the *same substrates* with *different catalysts* also resulted in a shift in the rate-limiting step and resting state of the catalyst. This highlights a further comparison to the Wilkinson's catalyst case studied by Halpern. Indeed, a multistep catalytic reaction mechanism has been compared by Collman, Hegedus, Norton, and Finke to a chameleon because of the way in which such differences can lead to subtle changes in the observed kinetics and mechanism.[2] Reaction progress kinetic analysis has the particular advantage of enabling the study of multistep reactions under conditions employing the "color of the chameleon" most likely to be synthetically meaningful.

Summary

This Perspective highlights how a new graphical methodology derived from reaction progress kinetic analysis provides a rapid and comprehensive global kinetic profile of complex catalytic reactions under practical synthetic conditions with a fraction of the number of experiments required by classical graphical approaches to catalytic reaction cycles. A series of examples from Pd-catalyzed coupling reactions of aryl halides demonstrates how the reaction orders in substrates and stability of the catalyst may be quantitatively determined even before proposing a reaction mechanism. To be considered plausible, any independent mechanistic proposal must be shown to be consistent with this global kinetic analysis. The advantage of this approach is that kinetic information rapidly obtained in this manner may then be used to inform the direction of mechanistic studies, providing a framework for further work seeking a molecular-level understanding of the nature of the species within the catalytic cycle.

Acknowledgment. Stimulating discussions with Prof. Stephen L. Buchwald, Dr. Eric R. Strieter, Mr. Timothy Barder, Prof. Andreas Pfaltz, Prof. Robert G. Bergman, Prof. David B. Collum, Prof. Barry K. Carpenter, and Dr. Chris Welch are gratefully acknowledged. Funding from the Max-Planck-Gesellschaft, the EPSRC, the UK Department of Trade and Industry "Manufacturing Molecules Initiative", Merck Research Laboratories, AstraZeneca, and Syngenta is gratefully acknowledged. We are grateful to two anonymous reviewers for thoughtful input. We thank Mr. Antonio Ferretti and Dr. Colin Ellis for experimental work. We thank Tim McKenna for the cover photo, in memory of Malik Joyeux.

References

(1) Halpern, J. *Inorg. Chim. Acta* **1981**, *50*, 11.
(2) Collman, J. P.; Hegedus, L. S.; J. R., N.; Finke, R. G. *Principles and Applications of Organotransition Metal Chemistry*; University Science Books: Sausalito, 1987.
(3) Blackmond, D. G. *Angew. Chem., Int. Ed.* **2005**, *44*, 4302.
(4) Heck, R. F. In *Comprehensive Organic Synthesis*; Trost, B. M., Fleming, I., Eds.; Pergamon: Oxford, New York, 1991; Vol. 4, p 833.
(5) de Meijere, A.; Meyer, F. E. *Angew. Chem., Int. Ed. Engl.* **1994**, *33*, 2379.
(6) Beletskaya, I. P.; Cheprakov, A. V. *Chem. Rev.* **2000**, *100*, 3009−3066.
(7) Muci, A. R.; Buchwald, S. L. *Top. Curr. Chem.* **2002**, *219*, 131.
(8) Hartwig, J. F. In *Handbook of Organopalladium Chemistry for Organic Synthesis*; Negishi, E. I., Ed.; Wiley-Interscience: New York, 2002; Vol. 1, p 1051.
(9) de Vries, A. H. M.; Mulders, J. M. C. A.; Mommers, J. H. M.; Henderickx, H. J. W.; de Vries, J. G. *Org. Lett.* **2003**, *5*, 3285.
(10) Herrmann, W. A.; Brossmer, C.; Reisinger, C. P.; Riermeier, T. H.; Oefele, K.; Beller, M. *Chem. Eur. J.* **1997**, *3*, 1357.
(11) Amatore, C.; Broeker, G.; Jutand, A.; Khalil, F. *J. Am. Chem. Soc.* **1997**, *119*, 5176.
(12) van't Hoff, J. H. *Etudes de dynamique chimique*; Muller: Amsterdam, 1884.
(13) Eadie, G. S. *J. Biol. Chem.* **1942**, *146*, 85.
(14) Hanes, C. S. *Biochem. J.* **1932**, *26*, 1406.
(15) Lineweaver, H.; Burk, D. *J. Am. Chem. Soc.* **1934**, *56*, 658.
(16) This is witnessed by the fact that the most-cited paper in the first 125 years of the *Journal of the American Chemical Society* is the Lineweaver−Burk paper describing linearization of the Michaelis−Menten equation (see *Chem. Eng. News*, **2003**, June 16, 27).
(17) Laidler, K. J. *Chemical Kinetics*, 3rd ed.; Harper Collins: New York, 1987.
(18) Steel, C.; Razi Naqvi, K. *J. Phys. Chem.* **1991**, *95*, 10713.
(19) Beezer, A. E. *Thermochim. Acta* **2001**, *380*, 205−208.
(20) Mathot, V. B. F. *Thermochim. Acta* **2000**, *355*, 1−33.
(21) Kemp, R. B.; Lamprecht, I. *Thermochim. Acta* **2000**, *348*, 1−17.
(22) Ferguson, H. F.; Frurip, D. J.; Pastor, A. J.; Peerey, K. M.; Whiting, L. F. *Thermochim. Acta* **2000**, *363*, 1.
(23) Regenass, W. *J. Thermal Anal.* **1997**, *49* 1661.
(24) Reaction rate is defined by rate $= 1/\nu_i \cdot 1/\mathrm{vol} \cdot d\xi/dt$; $\xi = (n_i - n_{i,0})/\nu_i$, where ξ is the extent of reaction, ν_i is the stoichiometric coefficient of species i, and n_i and n_{i0} are the moles of species i at time t and at time zero. Reaction rate and extent of reaction are species independent. These definitions hold for reactions exhibiting time-independent stoichiometry. A species-dependent rate may be defined for a constant volume system, where $n_i/\mathrm{vol} = C_i$, as *species rate* $= \nu_i \cdot$rate $= dC_i/dt$.
(25) Wang, J.; Sun, Y.; LeBlond, C.; Bradley, J. S.; Blackmond, D. G. *Studies in Surface Science and Catalysis*; Elsevier: Amsterdam, 1997.
(26) LeBlond, C.; Wang, J.; Blackmond, D.; Forman, A.; Larsen, R.; Orella, C.; Sun, Y. *Thermochim. Acta* **1996**, *289*, 189.
(27) Landau, R. N.; Singh, U. K.; Gortsema, F. P.; Gomolka, S. C.; Lam, T.; Futran, M.; Blackmond, D. G. *J. Catal.* **1995**, *157*, 201.
(28) The reaction vial is equilibrated in the calorimeter at reaction temperature until a stable baseline heat flow is obtained. Reaction is initiated by injection of one compound (in this case **1**) into a solution of the other components in solvent. Upon initiation, for a reaction exhibiting positive order kinetics the heat flow signal rises to its maximum value, with the first several data points occurring as the signal rises. The time lag through the reactor walls is accounted for by applying a time constant correction to the data.
(29) The parameter excess [*e*] is a constant when volume change is negligible over the course of the reaction. The mass balance given by eqs 5−7 holds when the concentration of any substrate-bound catalytic intermediates is small compared to the concentration of substrates.
(30) List, B.; Hoang, L.; Martin, H. J. *Proc. Natl. Acad. Sci. U.S.A.* **2004**, *101*, 5839−5842.
(31) Nyberg, A. I.; Usano, A.; Pihko, P. M. *Synlett* **2004**, 1891.
(32) Iwamura, H.; Blackmond, D. G. Unpublished data. A full mechanistic study will be reported in due course.
(33) Schultz, T. Ph.D. Thesis, Universität Basel, 2004.
(34) Rosner, T.; Le. Bars, J.; Pfaltz, A.; Blackmond, D. G. *J. Am. Chem. Soc.* **2001**, *123*, 1848.
(35) Mathew, J. S.; Blackmond, D. G.; Soheili, A.; Hughes, D.; Murry, J. Unpublished results. A full mechanistic study will be reported in due course.
(36) Mathew, J. S.; Ferretti, A.; Ashworth, I.; Brennan, C.; Blackmond, D. G. Unpublished results. A full mechanistic study will be reported in due course.
(37) Amatore, C.; Bensalem, S.; Ghalem, S.; Jutand, A.; Medjour, Y. *Eur. J. Org. Chem.* **2004**, 366.
(38) Shekhar, S.; Ryberg, P.; Hartwig, J. F. *Org. Lett.* **2006**, *8*, 851.
(39) Alcazar-Roman, L. M.; Hartwig, J. F.; Rheingold, A. L.; Liable-Sands, L. M.; Guzei, I. A. *J. Am. Chem. Soc.* **2000**, *122*, 4618.
(40) Alcazar-Roman, L. M.; Hartwig, J. F. *Organometallics* **2002**, *21*, 491.
(41) Ramachandran, B. R.; Halpern, A. M. *J. Chem. Educ.* **1996**, *73*, 689.
(42) For simplicity, we have omitted discussion of the role of base; however, in each of these four cases, we have shown the reaction to be zero order in base concentration, suggesting that the base is involved after the rate-limiting step in the cycle.
(43) In comparing reaction rates for stoichiometric steps with those for the global catalytic cycle, it is important to take into account concentration differences in the reacting catalytic species in the two cases. In Case I, the catalytic kinetics imply that the concentration of the oxidative addition complex I1 is very small and cannot be estimated with certainty.
(44) Singh, U. K.; Strieter, E. R.; Blackmond, D. G.; Buchwald, S. L. *J. Am. Chem. Soc.* **2002**, *124*, 14104.
(45) Shekhar, S.; Ryberg, P.; Hartwig, J. F.; Mathew, J. S.; Blackmond, D. G.; Strieter, E. R.; Buchwald, S. L. *J. Am. Chem. Soc.* **2006**, *128*, 3584.
(46) Cornish-Bowden, A. *Fundamentals of Enzyme Kinetics*; Portland Press: London, 1995.
(47) Van Strijdonck, G. F. P.; Boele, M. D. K.; Kamer, P. C. J.; de Vries, J. G.; van Leeuwen, P. W. N. M. *Eur. J. Inorg. Chem.* **1999**, 1073.
(48) It should be noted that the most recent stoichiometric studies of oxidative addition of PhBr to $Pd(binap)_2$ reported in ref 38 give values for k_{obs} that differ by a factor of 4 from the earlier reports in refs 39 and 40.
(49) Rosner, T.; Pfaltz, A.; Blackmond, D. G. *J. Am. Chem. Soc.* **2001**, *123*, 4621.
(50) Earlier catalytic data from ref 39 that appeared to support the on-cycle mechanism have since been found to be irreproducible.

JO052409I